Quasi-one-dimensional transport in the extreme quantum limit of heavily doped *n*-InSb

S. S. Murzin
Institute of Solid State Physics RAS, 142432, Chernogolovka, Moscow District, Russia

A. G. M. Jansen
Grenoble High Magnetic Field Laboratory, Max-Planck-Institut für Festkörperforschung and Centre National de la Recherche Scientifique, Boîte Postale 166, F-38042, Grenoble Cedex 9, France

E. G. Haanappel
Laboratoire de Physique de la Matière Condensée and Laboratoire National des Champs Magnétiques Pulsés, 143 Avenue de Rangueil, Boîte Postale 4245, 31432, Toulouse Cedex 4, France

(Received 30 November 1999; revised manuscript received 21 June 2000)

The longitudinal (ρ_{zz}) and transverse (ρ_{xx}) resistivities of heavily doped *n*-InSb have been studied systematically in the extreme quantum limit of applied magnetic field. The results are discussed in terms of the quasi-one-dimensional nature of the transport in the extreme quantum limit for the case of electron scattering by ionized impurities. The relation between transverse and longitudinal resistivity predicted for this case is verified experimentally both in magnetic-field and temperature-dependent data.

I. INTRODUCTION

The theoretical basis for electronic transport in the extreme quantum limit (EQL) of an applied magnetic field with only the lowest Landau level occupied was first given in the late 1950s. The description of magnetotransport in the lowest Landau-quantized state of the electrons[1–3] leads essentially to the same result for transverse and longitudinal conductivity as obtained for diffusional transport in the classical high-field case. However, in a quantum-mechanical description of the extreme quantum limit, the classical magnetotransport expressions will have to contain the magnetic-field dependence of the density of states and of the scattering rates.

Experimentally, the extreme quantum limit can be reached in metallically doped semiconductors. The doping element provides a free charge carrier to the otherwise (at low temperatures) insulating semiconductor, and acts, at the same time, as an ionized scattering center for charge carriers in these metallic systems. The above-cited theories are widely believed to give a correct description of magnetic-field-dependent transport in the extreme quantum limit (see various monographs and reviews[4–8]). However, it was realized that in the most interesting case of ionized impurities the electron interacts repeatedly with the same ionized impurities in quasi-one-dimensional motion along the magnetic field.[9–11] This leads to a breakdown of the diffusion over short distances perpendicular to the magnetic field. After a lateral displacement of the electron given by the screening length, diffusion describes the transport perpendicular to the magnetic field. For this modified diffusion a correlation can be derived between longitudinal and transverse conductivity which must be valid for applied magnetic fields in the extreme quantum limit up to the magnetic-field-induced metal-insulator transition.[11]

In Fig. 1, we give a schematic picture of the motion of the electrons to illustrate this modified transverse motion. Figure 1(a) shows the standard high-field diffusion of an electron at point-scattering impurities. For the case when the screening of the ionized impurities occurs on a length scale larger than the extent of the electronic wave function (i.e., the magnetic length), the scattering events are no longer independent, and the drift motion of the electrons is correlated for recurrent interactions with the same impurity potentials [see Fig. 1(b)]. We will discuss this correlated quasi-one-dimensional (1D) transport in more detail in Sec. II. The investigated topic is of relevance for investigations of quasi-1D conducting systems in zero magnetic field, because of the quasi-1D character of the transport in a 3D system in strong magnetic fields concerning the scattering with ionized impurities.

We have performed experiments on InSb samples with different electron concentrations in order to investigate this modified diffusion in the transverse magnetoconductivity related to quasi-one-dimensional magnetotransport in the ex-

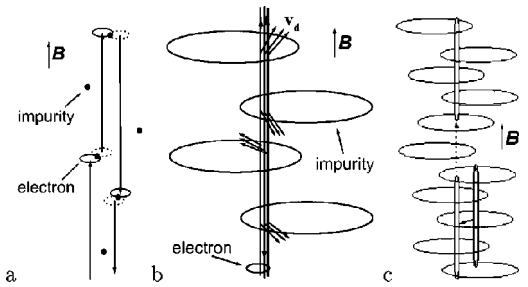

FIG. 1. (a) Electron diffusive motion in a high magnetic field due to point scattering by impurities. (b) Electron motion in a high magnetic field in the electric field of charged impurities. The electron returns many times in the same impurity potential, and drifts with the same velocity v_d. In the extreme quantum limit the screening length λ_s of the impurity potential is always larger than the magnetic length l_B (extent of the electronic wave function). (c) The motion of a quasilocalized electron in the extreme quantum limit. For some time the electron drifts across the magnetic field in the electric field of impurities (indicated by the small arrow), then hops into another drift trajectory (indicated by the dashed arrow).

treme quantum limit. The possibility to extend these experiments easily to magnetic fields up to 40 T and higher makes it worthwhile to reconsider the problem of magnetoquantum transport in the extreme quantum limit, which in itself dates back to the 1950s. Samples with higher charge-carrier densities can be investigated in the metallic state up to higher fields, without showing a magnetic-field-induced metal-insulator transition.

In magnetotransport investigations in the extreme quantum limit, two other issues will be considered. One is concerned with the change in regime of screening upon increasing the magnetic field. In the extreme quantum limit the electron wave vector $k_{z,F}$, parallel to the magnetic field, decreases with increasing magnetic field and can become smaller than the inverse screening length λ_s^{-1} which increases with magnetic field due to the increasing density of states at the Fermi level. This phenomenon reduces the scattering cross section of ionized impurities starting from a characteristic field ($k_{z,F} \simeq \lambda_s^{-1}$) and should lead to a nonmonotic field dependence of the longitudinal resistivity.[12] To our knowledge, this phenomenon has never been observed, because the magnetic-field-induced metal-insulator transition probably prevents the observation of such effects which are inherently connected to the metallic state of a system. In our experiments, we discuss this effect in view of an observed change in curvature in the field dependence of the longitudinal resistivity.

The second issue for quasi-one-dimensional transport in the EQL is related to localization phenomena for the situation when the transverse motion of the electrons is much smaller than the extent of the electronic wave function (the magnetic length) [see Fig. 1(c)]. If there is no transverse motion the electron is localized, because all electrons are localized even in weakly disordered 1D systems. A slow transverse motion results in a finite lifetime of the localized states, and the nonzero conductivity along the magnetic field is predicted to be much smaller compared to the standard Drude result.[13] We will consider this effect in our discussion of magnetotransport data in the extreme quantum limit. The most convincing indications of one-dimensional localization effects were found in the temperature dependence of the longitudinal transport along the magnetic field, which has an opposite temperature coefficient compared to the one expected for electron-phonon scattering.[12,14]

In the following we will present these different aspects related to quasi-one-dimensional motion in the extreme quantum limit. Experiments on metallically doped n-InSb will be presented and discussed in view of the above-sketched transport phenomena. The experimental data show the correlation between transverse and longitudinal conductivity as predicted for the recurrent interactions with ionized impurities. Such a correlation is seen both in the magnetic-field and temperature dependences of the transport data.

II. QUASI-1D MOTION IN THE EQL

The expressions for the magnetoconductivity in the extreme quantum limit of an applied magnetic field, with only the lowest Landau level occupied,[1–3] are not essentially different from the results for classically strong magnetic fields. The longitudinal conductivity σ_{zz} is described by the Drude formula

$$\sigma_{zz} = \frac{ne^2\tau_b}{m}, \tag{1}$$

where τ_b is the backward scattering time. The transverse conductivity is given by the Einstein relation

$$\sigma_{xx} = \nu_F e^2 D_{xx}, \tag{2}$$

which depends on the density of states at the Fermi level,

$$\nu_F = \frac{1}{(2\pi l_B)^2} \frac{\sqrt{2m}}{\hbar} \frac{1}{\sqrt{E_F}}, \tag{3}$$

and on the diffusion coefficient,

$$D_{xx} = \sum_i (\Delta x_i)^2 / 2\delta t, \tag{4}$$

in the plane perpendicular to the applied magnetic field B. Here $l_B = \sqrt{\hbar/eB}$ is the magnetic length. The Fermi energy E_F is taken from the energy of the lowest Landau level, so that $E = \hbar^2 k_z^2/2m$ is the energy related to the electron motion along the magnetic field. In the extreme quantum limit, $E_F \propto B^{-2}$ holds if one neglects the dependence of the effective mass m on the magnetic field. The summation in Eq. (4) is performed over all collisions experienced by an electron during a long time-interval δt, where Δx_i is the change in the x coordinate of an electron as a result of the ith collision. In Fig. 1(a) we schematically sketch the diffusion in strong fields with point scattering at impurities. The results for the conductivity tensor differ from the classically strong-magnetic-field case in the magnetic-field dependence of the density of states ν_F and of the scattering times only. These dependences of scattering times are different for different scattering mechanisms. For our doped semiconductor samples, the dominant scattering mechanism is scattering by ionized impurities.

The above given description has been generally accepted for a long time, with quotations in various reviews and monographs.[4–8] However, because of the quasi-one-dimensional electron motion, expressions (1) and (4) do not apply to the most interesting case of scattering by ionized impurities, from an experimental point of view. That is, in the extreme quantum limit, during the backward scattering time τ_b, the displacement $r_\perp$ of electrons perpendicular to the magnetic field is smaller than the screening length λ_s and the magnetic length l_B. In the EQL,

$$r_\perp < l_B < \lambda_s. \tag{5}$$

To show this, the displacement $r_\perp$ in a time τ_b can be estimated by using the expression $r_\perp = \sqrt{D_{xx}\tau_b}$ with D_{xx} and τ_b obtained in Refs. 1 and 2 for the EQL:

$$r_\perp \sim l_B^2 \sqrt{4k_{z,F}^2 + \lambda_s^{-2}} < l_B. \tag{6}$$

$r_\perp$ is always smaller than l_B in the extreme quantum limit, because $l_B k_{z,F} = \sqrt{2E_F/\hbar\omega_c} < 1$ and $l_B \lambda_s^{-1} < 1$ ($k_{z,F}$ is the

Fermi wave number of the electrons at the Fermi energy, and $\omega_c = eB/m$ is the cyclotron frequency). The last inequality follows from

$$\lambda_s = (e^2 \nu_F / \epsilon\epsilon_0)^{-1/2} = l_B \sqrt{\pi^3 n a_B l_B^2} > l_B \tag{7}$$

for a metallic system with $n a_B l_B^2 > 1$. Here ϵ is the relative dielectric constant of the lattice, and $a_B = 4\pi\hbar^2 \epsilon\epsilon_0 / me^2$ the Bohr radius.

For the case $r_\perp \ll \lambda_s$ in the EQL, we cannot consider all scattering events as independent, and expression (4) is not valid. Especially for this case of a quasi-one-dimensional random walk along the magnetic field, an electron scattered once by an ionized impurity will return many times into an electric field of the same impurity before it moves across the magnetic field through a distance $\sim\lambda_s$ [see Fig. 1(b)]. For each interaction with the electric field of the impurity under examination, the electron will drift in crossed fields (the electric field of the impurity and the external magnetic field) in, approximately, the same direction over a length $a \ll \lambda_s$. If the electron interacts M times with P impurities during the time interval δt, the diffusion coefficient equals

$$D_{xx} \approx \frac{\sum_{i=1}^{P} \left(\sum_{j=1}^{M} \Delta x_{i,j} \right)^2}{2\,\delta t} \approx \frac{a^2}{\delta t} P M^2. \tag{8}$$

This diffusion coefficient is M times larger than the one obtained under the assumption of independent scattering events, where

$$D_{xx} \approx \frac{\sum_{i,j} (\Delta x_{i,j})^2}{2\,\delta t} \approx \frac{a^2}{\delta t} P M. \tag{9}$$

The transverse motion of an electron has a nondiffusive nature over a distance shorter than λ_s, and becomes diffusive only over a length scale greater than λ_s. The characteristic step of such a diffusion is of the order of λ_s, and the diffusion coefficient is $D_{xx} \sim \lambda_s^2 / t_s$, where t_s is the time over which the electron is displaced over a distance $\sim\lambda_s$. The time t_s depends on the probability of the electron motion to return to an electric field of the same impurity and, therefore, depends on the diffusion D_{zz} along the magnetic field.

The scenario given above was worked out in Refs. 9 and 10. In Ref. 11, the following correlation was derived between the transverse and longitudinal conductivity:

$$\sigma_{xx} = \alpha \left(\frac{e^3 \nu_F}{4\pi\epsilon\epsilon_0 B} \right)^{4/3} N^{2/3} \lambda_s^{2/3} \sigma_{zz}^{-1/3}, \tag{10}$$

where N is the density of ionized impurities, and α a numerical coefficient of order unity. The presence of σ_{zz} in the right part of Eq. (10) follows from the dependence of the number M, i.e., the number of correlated drift interactions of an electron with one impurity in Eq. (8), on the diffusion coefficient along the magnetic field $D_{zz} = \sigma_{zz} / e^2 \nu_F$. Using the Hall conductivity $\sigma_{xy} = ne/B \gg \sigma_{xx}$, this relation can be rewritten for the transverse ($\rho_{xx} = \sigma_{xx} / \sigma_{xy}^2$) and longitudinal ($\rho_{zz} = 1/\sigma_{zz}$) resistivities as

$$\rho_{xx} = \frac{\alpha}{4^{7/3}\pi^{13/3}} \frac{m e^{10/3} B^{8/3}}{n^{7/3} \hbar^4 \epsilon\epsilon_0} \rho_{zz}^{1/3} \left(\frac{N}{n} \right)^{2/3}, \tag{11}$$

with the expressions for density of states ν_F and screening length in the extreme quantum limit. There is no such a universal correlation between σ_{xx} and σ_{zz} in the standard description of Adams and Holstein. In the Adams-Holstein theory,[2] for almost all scattering mechanisms one obtains $\rho_{xx} \propto B^3 \rho_{zz}$. Only for scattering with ionized impurities, $\rho_{xx} \propto \rho_{zz}$ for the case $k_{z,F} \lambda_s \gg 1$. These relations follow from a comparison of the two independent transport equations for longitudinal and transverse motion in the Adams-Holstein theory. We note that Eq. (10) is valid whenever the electron displacement across the magnetic field during the backflow time along the magnetic field is smaller than the screening length ($r_\perp \ll \lambda_s$), even for classically strong magnetic fields in the absence of Landau quantization.

Upon increasing the magnetic field in the EQL, the wave vector $k_{z,F}$ decreases ($\propto B^{-1}$), and the screening increases due to the increasing density of states at the Fermi level [see Eq. (7)]. A transition occurs from a classical screening $k_{z,F}\lambda_s > 1$ to a quantum-mechanical screening $k_{z,F}\lambda_s < 1$. As a result the backscattering along the magnetic field changes slope with magnetic field, and a maximum is expected in the field dependence of ρ_{zz}.[12] The observed change in curvature of $\rho_{zz}(B)$ in our measurements could be a precursor for such a maximum which has never been observed.

For $r_\perp$ much smaller than l_B, localization effects should influence the one-dimensional transport of the longitudinal conductivity[11,13,15] because l_B determines the extent of the wave function of electrons across the magnetic field in the extreme quantum limit. It is well known that all electrons in disordered 1D systems are localized regardless of their energy.[16,17] If there were no transverse motion at all, the electron would be localized along the field direction because of the one-dimensional nature of the motion, as shown schematically in Fig. 1(c). A slow transverse motion results in a finite lifetime of the localized states and a nonzero conductivity along the magnetic field, which will be considerably smaller than the Drude formula [Eq. (1)] predicts. For the cases $k_{z,F}\lambda_s \gg 1$ and $k_{z,F} l_B \ll 1$, Ref. 13 derived the result

$$\sigma_{zz} \sim \frac{n e^2 \tau_b}{m} (k_{z,F} l_B)^2 \ln(1/2 k_{z,F} l_B). \tag{12}$$

A qualitative interpretation of this result was given in Ref. 11. In Ref. 15 the case of a smooth potential was considered on the basis of the approach for the one-dimensional case,[17] and the same result [Eq. (12)] without logarithmic factor was obtained.

Because of the unchanged correlation between longitudinal and transverse transport, expressions (10) and (11) are valid for one-dimensional transport both when 1D localization effects are important and when they are not. 1D localization effects, leading to a decrease of the longitudinal conductivity, result in an increase of the transverse conductivity. With increasing temperature, the suppression of localization effects should lead to an increase in the longitudinal conductivity and, according to Eq. (10), to a decrease of the transverse conductivity. This phenomenon was observed in the temperature dependence of magnetotransport experiments on

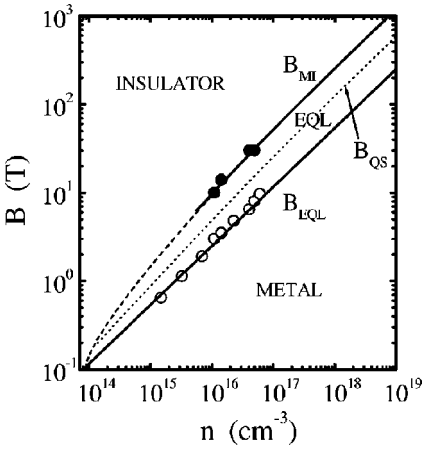

FIG. 2. Experimental data (circles) and calculated dependencies (lines) of the fields B_{EQL}, B_{QS}, and B_{MI} for the extreme quantum limit, the quantum screening and the metal-insulator transition as a function of the electron density n, respectively.

InAs and InSb,[14] with $\rho_{xy} \gg \rho_{xx}$, ρ_{zz}, and ρ_{xy} practically independent of temperature. We note that in the frame of work Adams-Holstein theory,[2] the temperature dependence of the resistivity can be caused by the electron-phonon scattering only. It leads exactly to the opposite behavior. Here an increase of temperature decreases the longitudinal conductivity, and increases the transverse conductivity.

Besides localization, electron-electron interaction also plays an important role in the extreme quantum limit. Due to the strongly reduced diffusion perpendicular to the magnetic field, the electron-electron-interaction quantum corrections to the diagonal components of the conductivity tensor increase with the magnetic field,[18] and can be shown to become comparable to the conductivity itself.[19,20] The electron-electron interaction effects make the dominant contribution to the temperature dependence at low temperatures. An indication of such a phenomenon was found in the observed decrease of both the longitudinal and transverse conductivity at low temperatures ($T<1$ K) while the Hall conductivity is independent of temperature,[20] and in the violation of relations (10) and (11). For the investigations above 1.5 K presented here, we will not consider this phenomenon.

In this work we study the longitudinal (ρ_{zz}) and transverse (ρ_{xx}) magnetoresistivities of heavily doped n-InSb with different electron densities in the extreme quantum limit of the applied magnetic field, in order to explore the existence of one-dimensional transport. One of the proofs for such quasi-one-dimensionality is given by an experimental verification of the relation between ρ_{zz} and ρ_{xx} in Eq. (11).

III. SAMPLES

In order to study the magnetotransport properties in the extreme quantum limit with only the lowest Landau level occupied, we have investigated the metallically doped semiconductor InSb. The extreme quantum limit starts at the field B_{EQL} of the last Shubnikov–de Haas oscillation, and the metallic regime finishes at the magnetic-field-induced metal-insulator transition at the field B_{MI}.

In Fig. 2 we plot (open circles) the fields of the last minimum in the Shubnikov–de Haas structures of ρ_{xx} as a function of the electron density n of different samples (not all these samples have been investigated in detail in the present investigation). These experimental data can be compared very well with the B_{EQL} values (lower solid line), as deduced from the condition $E_F = g^* \hbar \omega_c/2$, yielding

$$B_{EQL} = 2^{2/3} \pi^{4/3} \frac{\hbar}{e} \frac{n^{2/3}}{|g^*|^{1/3}}. \tag{13}$$

Here $g^* \equiv g m/m_e = -0.71$ is the effective g factor of InSb with the effective mass $m = 0.014 m_e$ near the conduction-band bottom (m_e is the free-electron mass).

For an uncompensated semiconductor the metal-insulator transition field B_{MI} is determined by the reduced overlap of the electronic wave functions in a magnetic field via the condition[21,22]

$$n a_{\parallel} a_{\perp}^2 = \delta, \tag{14}$$

where $a_{\parallel} = 2 a_B / \ln(a_B/l_B)$ and $a_{\perp} = 2 l_B$. However, the exact value of δ is unknown. For our samples, we have defined the field B_{MI} as the field, where $d \log \rho_{xx}/d \log B$ starts to change at low temperatures (down to 50 mK; see Fig. 4 below) accompanied by a strong temperature dependence of all components of the resistivity tensor. The experimental data can be fitted by Eq. (14) with $\delta \approx 0.04$ (see Fig. 2). Equation (14) is valid only when a_B/l_B at the field B_{MI} is rather large [the solid high-field part of the curve for $B_{MI}(n)$ in Fig. 2]. The dashed part is a schematic prolongation of B_{MI} using the expression $n_c a_B^3 = 0.027$ of the metal-insulator transition in zero magnetic field at the critical electron density n_c.[23] In these calculations the magnetic field dependence of the effective electron mass due to the nonparabolicity of the conduction band in InSb was taken into account using the two-band model[24]

$$m(B) = m \sqrt{1 + 2 \frac{\hbar \omega_c (1 - |g^*|/2) + k_{z,F}^2 \hbar^2/m}{E_g}}, \tag{15}$$

where $E_g = 236$ meV is the band gap. These corrections in the effective mass are about 40% for a 20-T field, and were verified in magneto-optical experiments.[25]

Near the field B_{EQL} the screening is classical ($k_{z,F} \lambda_s \gg 1$) if $|g^*| \sim 1$. With increasing field $k_{z,F} \lambda_s$ decreases, and the screening requires a quantum-mechanical description of an impurity potential at $k_{z,F} \lambda_s < 1$.[12] The field B_{QS}, which divides classical and quantum screening regions, as defined by the relation $2 k_{z,F} \lambda_s = 1$, is plotted in Fig. 2 as a function of n by the dotted line.

The dependencies of the characteristic fields as a function of electron density in Fig. 2 show that the relative magnitude B_{MI}/B_{EQL} of the characteristic fields does not really increase for electron densities above 5×10^{16} cm^{-3}. Therefore, the characteristic parameter $r_{\perp}/l_B$ for the importance of 1D transport in the metallic region above B_{EQL} does not strongly decrease with increasing electron concentration.

We have investigated the magnetotransport in the extreme quantum limit for different InSb samples (Nos. 1–5) with electron densities $n = 1.1$, 1.4, 2.3, 4.1, and 5.0 $\times 10^{16}$ cm^{-3} and with mobilities μ of 12, 12, 10, 8.2, and 8.3×10^4 cm^2/V s, respectively (values at 4.2 K). The

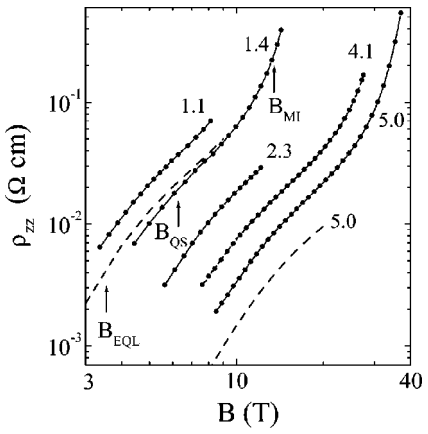

FIG. 3. Longitudinal magnetoresistance ρ_{zz} in the extreme quantum limit of the applied magnetic field at $T \approx 1.5$ K for InSb samples with different electron densities (solid circles). The numbers near the curves indicate the electron densities in units 10^{16} cm^{-3}. The dashed lines show magnetoresistance calculations for the samples with the smallest (upper line) and the largest (lower line) electron density. The arrows indicate the field B_{EQL} for the extreme quantum limit, field B_{QS} for quantum screening, and field B_{MI} for the metal-insulator transition for sample No. 2, with an electron density 1.4×10^{16} cm^{-3}.

single-crystalline samples were in most cases cut by spark erosion in a Hall-bar geometry with legs for the voltage measurements. Before contacting the samples, they were etched with SR-4A etchant. The dimensions of the samples were of the order of 1 mm^2 in cross section and 10 mm in length. The mobilities of the samples are close to the mobilities of the best samples of this kind of crystals with comparable electron densities. Since the residual density of acceptors is only about 10^{14} cm^{-3}, the InSb are practically uncompensated, i.e., the impurity concentration N equals the carrier concentration n. The zero-magnetic-field resistivity of the investigated samples depends very weakly on temperature.

The quality of the current contacts is very important for longitudinal resistivity measurements because of the strong anisotropy of the conductivity parallel and perpendicular to the magnetic field. The indium current contacts have to cover the surface of the end faces of the sample entirely. In many cases the quality of the contacts was not good enough, as manifested in the experiments by a linear magnetoresistance in weak magnetic fields and by a singularity in the longitudinal magnetoresistance when the Fermi level coincides with the bottom of the spin-split Landau subband 0^-. This singularity should not arise in the longitudinal magnetoresistance, because the component of the velocity parallel to the field tends to zero at the bottom of the 0^- minority-spin subband, and spin-flip scattering is absent between the two lowest spin-split Landau levels 0^+ and 0^-. In cases when the contact quality was unsatisfactory, new contacts were fabricated. The transverse resistance measurements were carried out by the four-terminal method. The longitudinal resistance measurements were carried out by both the four-terminal method and the two-terminal method (the voltage between current contacts was measured). For good contacts the results were independent of the contact configuration. The measurements of the longitudinal resistance of the two samples with the highest electron density were carried out in a pulsed magnet using the two-terminal method.

IV. EXPERIMENTAL RESULTS AND DISCUSSION

A. Longitudinal magnetoresistance

In Fig. 3 the longitudinal magnetoresistivity ρ_{zz} is plotted for all our samples at $T \approx 1.5$ K. The experimental data are plotted in the extreme quantum limit starting from the fields near the last minimum of the Shubnikov–de Haas oscillations in $\rho_{xx}(B)$, where the extreme quantum limit starts (indicated by the arrow with B_{EQL} for one of the samples in Fig. 3). At higher magnetic fields the strong upturn in $\rho_{zz}(B)$ corresponds to the magnetic-field-induced metal-insulator transition (indicated by arrow with B_{MI}).

From the magnetic-field dependence of $\rho_{zz}(B)$ it follows that the derivative $d\ln\rho_{zz}/d\ln B$ changes nonmonotonically with the field. Initially it decreases, then increases again. To our knowledge such a behavior has not been reported before. For an explanation of such a behavior of $\rho_{zz}(B)$, we consider the influence of screening on the backward scattering time τ_b in the extreme quantum limit. In accordance with the very first estimates,[1] and given that the real part of the dielectric function of the electron system has a logarithmic Kohn singularity at wave number $2k_{z,F}$,[26] which is spread by the broadening of the electronic states by the amount $\Gamma = \hbar/\tau_f + \hbar/\tau_b$,[27] the forward and backward scattering times can be written as

$$\frac{1}{\tau_b} = 8\pi\frac{E_B}{\hbar}\frac{Nl_B^2}{k_{z,F}}\Phi_0(\xi), \quad \text{and} \quad \frac{1}{\tau_f} = 8\pi\frac{E_B}{\hbar}\frac{Nl_B^2}{k_{z,F}}\Phi_0(\xi'). \tag{16}$$

The forward scattering involves scattering without a change in the momentum of the electron along the magnetic field. $E_B = me^4/32\pi^2\epsilon^2\epsilon_0^2\hbar^2$ is the Bohr energy, and

$$\Phi_n(\xi) = \int_0^\infty \frac{x^n e^{-x}}{(x+\xi)^2}, \tag{17}$$

$$\xi = 0.5[4k_{z,F}^2 + \lambda_s^{-2}\ln(8E_F/\Gamma)/2]l_B^2, \quad \xi' = 0.5\lambda_s^{-2}l_B^2.$$

For the case of a good metal ($na_Bl_B^2 \gg 1$) in high magnetic fields, when $\xi \ll 1$,

$$\frac{1}{\tau_b} = 16\pi\frac{E_B}{\hbar}\frac{N}{k_{z,F}[4k_{z,F}^2 + \lambda_s^{-2}\ln(8E_F/\Gamma)/2]}. \tag{18}$$

Since both $k_{z,F}$ and λ_s are propotional to $1/B$ in the extreme quantum limit, expression (18) clearly shows that the magnetic-field dependence of τ_b and, correspondingly, that of ρ_{zz}, are different in the classical screening region ($k_{z,F}\lambda_s \gg 1$) compared to the quantum screening region ($k_{z,F}\lambda_s \ll 1$). The longitudinal magnetoresistivity calculated with the help of Eq. (18) should increase, then decrease, in the quantum screening region before finally increasing again at the metal-insulator transition. Even if localization effects are important, the expected qualitative behavior of ρ_{zz} would be the same.[12] Such a nonmonotonic behavior of ρ_{zz} would be expected if the field B_{QS} is much larger than B_{EQL} and much smaller than B_{MI}. In our samples the field B_{EQL} is a

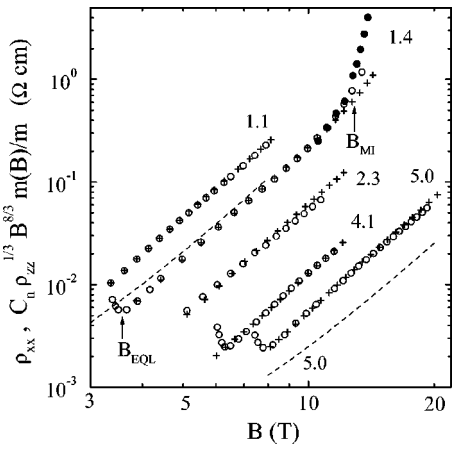

FIG. 4. Transverse magnetoresistance ρ_{xx} (open circles) and rescaled longitudinal magnetoresistance $C_n B^{8/3} \rho_{zz}^{1/3} m(B)/m$ (crosses) at $T \approx 1.5$ K for different samples with indicated electron concentration (units 10^{16} cm^{-3}). For sample No. 2, ρ_{xx} is also presented at $T = 80$ mK to indicate the field B_{MI}. The dashed lines show calculations using the Adams-Holstein theory for the samples with the smallest and largest electron densities. The arrows indicate the estimated fields B_{EQL}, and B_{MI} for sample No. 2.

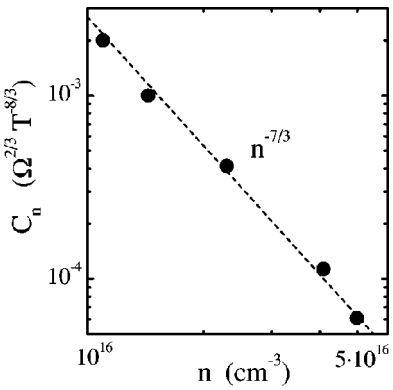

FIG. 5. The coefficients C_n obtained from the data analysis in Fig. 4 as a function of the electron density. The dashed line shows the dependence $C_n \propto n^{-7/3}$.

few times smaller than B_{MI}, and the field B_{QS} is close to B_{MI} (see Fig. 2). Therefore, probably as a signature of this effect, only a decrease in $d \ln \rho_{zz}/d \ln B$ is observed.

For a comparison with experimental data, we have calculated ρ_{zz} as a function of the magnetic field using Eqs. (16) and (17). The nonparabolicity of the conduction band results in a dependence of the effective mass on the magnetic field [Eq. (15)], and was taken into account for this calculation. Since τ_b enters the right-hand side of Eq. (16) through the τ_b dependence of Γ or $\Phi_0(\xi)$, Eqs. (16) and (17) were solved by an iterative method. In first approximation we took λ_s^{-2} instead of $\lambda_s^{-2} \ln(8E_F/\Gamma)$ in Eq. (17). Subsequently, we substituted the obtained values of τ_b and τ_f in Γ, and so on. Already after three iterations a good convergence was obtained. For the two samples with the highest and lowest charge-carrier concentrations, the calculated data for $\rho_{zz}(B)$ are plotted as the dashed curves in Fig. 3. The calculated values are approximately two times smaller than the experimental measurements. The given calculations should be taken with care. The calculations are fairly adequate for the initial sections of the curves, where $E_F \tau_b/\hbar \gg 1$ as holds for a metallic system. For example, for sample No. 5, $E_F \tau_b/\hbar = 23$ in a 9-T field. As $E_F \propto B^{-2}$ and τ_b decreases quickly with the magnetic field, the parameter $E_F \tau_b/\hbar$ becomes about unity in a field $2B_{EQL}$. Moreover, in larger fields close to the metal-insulator transition, Eqs. (16) and (17) are no longer valid.

The difference in ρ_{zz} between theory and experiment could be ascribed to the above-mentioned 1D localization effects, which were not taken into account in the calculations. Existing theories for localization effects in the longitudinal transport[13] cannot be used for the calculation of ρ_{zz} in our case, because they have been developed for conditions $k_{z,F} \lambda_s \gg 1$ and $k_{z,F} l_B \ll 1$, which are not well realized. The parameter $r_\perp/l_B$, which determines the importance of localization effects, is not very small. For sample No. 5, for example, in a 15-T field $r_\perp = 3.8 \times 10^{-7}$ cm and $l_B = 6.6 \times 10^{-7}$ cm. Therefore, the localization effects should not be very large. One can expect that they change resistivity only a few times. We note that the most convincing indications of one-dimensional localization effects were found in the temperature dependence of ρ_{zz}, which is totally different from the one expected for electron-phonon scattering,[14,12] as will be presented below.

B. Transverse magnetoresistance

In Fig. 4 we plot the transverse magnetoresistivity ρ_{xx} as a function of magnetic field at $T \approx 1.5$ K. For sample No. 2, we have again indicated the characteristic fields B_{EQL} (minimum in ρ_{xx}) and B_{MI}. The existence of the metal-insulator transition is demonstrated by the added data at 80 mK for sample No. 2, showing a stronger upturn at lower temperatures.

With the appropriate choice of coefficients C_n, Fig. 4 contains the rescaled data $C_n B^{8/3} \rho_{zz}^{1/3} m(B)/m(0)$ of the longitudinal resistance. The coefficients C_n were chosen in order to have a good overlap with the $\rho_{xx}(B)$ data. A good agreement is found with the expected dependence for the correlation between longitudinal and transverse transport according to Eq. (10). The data for sample No. 3, with an electron density 2.3×10^{16} cm^{-3}, do not show such a good agreement. For this sample, the measured transverse resistance was different for the two different magnetic-field polarities (about a factor 2 in the smallest fields, and about 5% at the highest). In Fig. 4 we plot the average of the two field polarities. Probably even the average does not give a correct measurement of ρ_{xx}, which could explain the deviation observed in Fig. 4 for sample No. 3.

In Fig. 5 we plot the coefficients C_n as a function of the electron concentration n. The best linear fit for the dependence of $\log C$ on $\log n$ gives a power-law dependence $C_n \propto n^q$ with $q = -2.24 \pm 0.07$. This dependence is very close to the expected power $-7/3 = -2.33$ according to Eq. (10). The deduced numerical coefficient α in Eqs. (10) and (11) equals $\alpha = 2.1$.

In Fig. 4 we plot the calculated $\rho_{xx} = \sigma_{xx}/\sigma_{xy}^2$ using the Adams-Holstein theory[2]

$$\sigma_{xx} = 2\pi e^2 \nu_F \frac{E_b}{\hbar} \frac{N l_B^4}{k_{z,F}} [\Phi_1(\xi) + \Phi_1(\xi')]. \qquad (19)$$

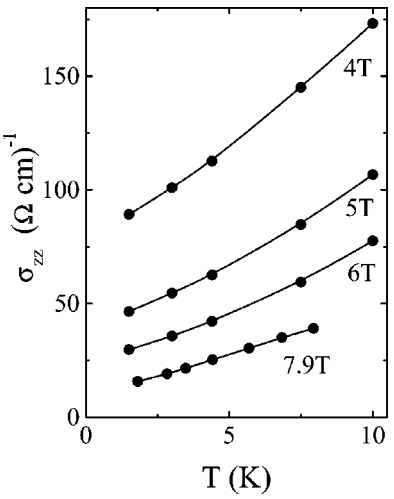

FIG. 6. Temperature dependences of the longitudinal conductivity σ_{zz} for sample No. 1 for the indicated magnetic fields in the extreme quantum limit.

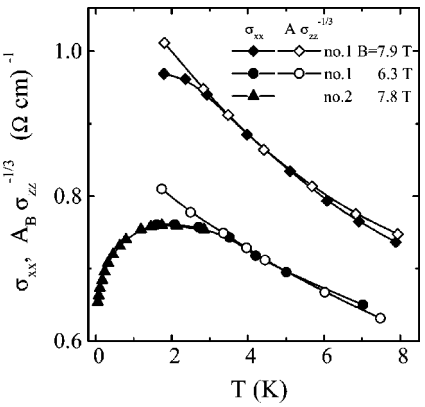

FIG. 7. Temperature dependences of the transverse conductivity σ_{xx} and of $A\sigma_{zz}^{-1/3}$ for sample No. 1 at two different magnetic fields. The fit coefficients A are different for different curves. For sample No. 2 we show the σ_{xx} data down to 50 mK, showing strong electron-electron-interaction effects (see the text).

The calculated values of ρ_{xx} are 2–3 times smaller than the experimental values. The correlations in the electron scattering across the magnetic field, as discussed in Fig. 1(b), increase the diffusion coefficient D_{xx}, and therefore the resistivity $\rho_{xx} \propto D_{xx}$. Since l_B and $r_\perp$ are not very small with respect to λ_s (for sample No. 5 in a 15-T field, $l_B = 6.6 \times 10^{-7}$ cm, $r_\perp = 3.8 \times 10^{-7}$ cm, and $\lambda_s = 12.4 \times 10^{-7}$ cm), one can expect that the correlated scattering increases the resistivity only a few times. In the lower field range, where the Fermi energy is large and therefore the standard theories[2,11] can be better applied, the calculated magnetic, field dependence using the Adams-Holstein theory[2] is weaker than observed in the experimental data.

C. Temperature dependence

The longitudinal conductivity σ_{zz} of our samples increases with increasing temperature, as shown in Fig. 6 for sample No. 1 for different fields in the extreme quantum limit. This is opposite to the expected influence of electron-phonon scattering. With increasing temperature, the transverse conductivity σ_{xx} increases up to 1 K and decreases above 2 K (see Fig. 7). In this high-temperature region $\sigma_{xx}(T) \propto \sigma_{zz}(T)^{-1/3}$ holds, in accordance with Eq. (10). The Hall conductivity σ_{xy} is practically independent of temperature in the presented temperature range. The temperature-dependent data above 2 K with the observed correlation between longitudinal and transverse transport give strong evidence for the importance of quasi-one-dimensional effects in the electron transport in strong magnetic fields. At lower temperatures, below 1 K, a strong decrease in σ_{xx} is observed, as illustrated in Fig. 7, with data down to 50 mK for sample No. 2. The relation between longitudinal and transverse conductivity components [Eq. (10)] breaks down in this temperature range. Electron-electron-interaction effects have been put forward for the explanation of this phenomenon.[20]

In summary, the magnetic-field and temperature dependence of the resistivities ρ_{zz} and ρ_{xx} of the investigated metallically doped InSb samples show a correlated behavior between longitudinal and transverse resistance in the extreme quantum limit. The correlation can be described by a model as derived for the quasi-1D motion of the electrons in a strong magnetic field. Although the possible existence of localization effects in the quasi-1D transport does not allow for a detailed theoretical description of the experimental magnetotransport data, the universal relations between ρ_{zz} and ρ_{xx} [Eqs. (10) and (11)] are confirmed experimentally. By comparing different samples, the expected concentration dependence in the correlated transport is found. The most striking experimental result which would support the developed concept of a 1D localization phenomenon along the magnetic field is the observed temperature dependence of σ_{zz} and σ_{xx}, which is just opposite to what is expected for electron-phonon scattering in the standard approach of Adams and Holstein.

ACKNOWLEDGMENTS

This work was supported by RFBR-PICS (Grant No. 98-02-22037) and the program ''Physics of Solid State Nanostructures'' (Grant No. 99-1127).

[1] P.N. Argyres and E.N. Adams, Phys. Rev. **104**, 900 (1956).
[2] E.N. Adams and T.D. Holstein, J. Phys. Chem. Solids **10**, 254 (1959).
[3] R. Kubo, H. Hasegawa, and N. Hashitdume, J. Soc. Jpn. Phys. **14**, 56 (1959).
[4] R. Kubo, S. J. Miyake, and N. Hashitdume, Solid State Physics Vol. 17, edited by F. Seitz and D. Turnbull (Academic Press, New York, 1965), p. 269.
[5] L. M. Roth and P. N. Agryes, in *Physics of III-V Compounds*, Semiconductors and Semimetals Vol. 1, edited by R. K. Willardson and A. C. Beer (Academic Press, New York, 1966), p. 159.

[6] J. Hajdu and G. Landwehr, Topics in Applied Physics Vol. 57, edited by F. Herlach (Springer-Verlag, Berlin, 1985).
[7] V. F. Gantmakher and Y. B. Levinson, in *Modern Problems in Condensed Matter Sciences*, edited by V. M. Agranovich and A. A. Maradudin (North-Holland, Amsterdam, 1987), Vol. 19.
[8] J. Hajdu and G. Landwehr, in *Landau Level Spectropy*, edited by G. Landwehr and E. I. Rashba (Elsevier, Amsterdam, 1991), Vol. 57, p. 997.
[9] S. S. Murzin, Pis'ma Zh. Éksp. Teor. Fiz. **39**, 567 (1984) [JETP Lett. **39**, 695 (1984)].
[10] D. G. Polyakov, Zh. Éksp. Teor. Fiz. **90**, 546 (1986) [Sov. Phys. JETP **63**, 317 (1986)].
[11] S. S. Murzin, Pis'ma Zh. Éksp. Teor. Fiz. **45**, 228 (1987) [JETP Lett. **45**, 283 (1987)].
[12] V. V. Kosarev, N. A. Red'ko, and V. I. Belitskiĭ, Zh. Éksp. Teor. Fiz. **100**, 492 (1991) [Sov. Phys. JETP **73**, 270 (1991)].
[13] A. A. Abrikosov and I. A. Ryzhkin, Fiz. Tverd. Tela (Leningrad) **19**, 59 (1978) [Sov. Phys. Solid State **19**, 33 (1977)]; Adv. Phys. **27**, 405 (1979).
[14] F. A. Egorov and S. S. Murzin, Zh. Éksp. Teor. Fiz. **94**, 315 (1988) [Sov. Phys. JETP **67**, 1045 (1988)].
[15] D. G. Polyakov, in *Proceedings of the 20th International Conference on Semiconductors, Greece*, 1990, edited by E. M. Anastassakis and J. D. Joannopoulos (World Scientific, Singapore, 1990), p. 2321.
[16] N. F. Mott and W. D. Twose, Adv. Phys. **10**, 107 (1961).
[17] V. L. Berezinsky, Zh. Éksp. Teor. Fiz. **65**, 1251 (1973) [Sov. Phys. JETP **38**, 620 (1974)].
[18] B. L. Al'tshuler and A. G. Aronov, Zh. Éksp. Teor. Fiz. **77**, 2028 (1979) [Sov. Phys. JETP **50**, 486 (1979)].
[19] S. S. Murzin, Pis'ma Zh. Éksp. Teor. Fiz. **44**, 45 (1986) [JETP Lett. **44**, 56 (1986)].
[20] S. S. Murzin and A. G. M. Jansen, J. Phys.: Condens. Matter **4**, 2201 (1992).
[21] Y. Yafet, R. W. Keyes, and E. N. Adams, J. Phys. Chem. Solids **1**, 137 (1956).
[22] B. I. Shklovskii and A. L. Efros, *Electronic Properties of Doped Semiconductors* (Springer-Verlag, Berlin, 1984).
[23] N. F. Mott and E. A. Davis, *Electron Processes in Non-Crystalline Materials* (Clarendon Press, Oxford, 1979).
[24] E. O. Kane, J. Phys. Chem. Solids **1**, 249 (1957).
[25] E. D. Palik and G. B. Wright, in *Optical Properties of III-V Compounds*, Semiconductors and Semimetals Vol. 3, edited by R. K. Willardson and A. C. Beer (Academic Press, New York, 1967), p. 421.
[26] N. J. Horing, Ann. Phys. (N.Y.) **54**, 405 (1969).
[27] U. Paulus and J. Hajdu, Solid State Commun. **20**, 687 (1976).